

High efficiency n-type Metal-Wrap-Through cells and modules using industrial processes

N. Guillevin^a, I.G. Romijn^a, L.J. Geerligs^a, B.B Van Aken^a, I.J. Bennett^a, M.J. Jansen^a, Wang jianming^b, Wang ziqian^b, Zhai jinye^b, Wan zhiliang^b, Tian shuquan^b, Zhao wenchao^b, Hu zhiyan^b, Li gaofei^b, Yu bo^b, Xiong jingfeng^b

^aECN Solar Energy, P.O. Box 1, NL-1755 ZG Petten, the Netherlands - email: guillevin@ecn.nl
^bYingli Green Energy Holding Co.,Ltd. 3399 North Chaoyang Avenue, Baoding, China.

Abstract

We report on our high efficiency n-type metal-wrap-through (MWT) cell and module technology. In this work, bifacial n-type MWT cells are produced by industrial processes in industrial full-scale and pilot-scale process equipment. N-type cells benefit from high recombination lifetime in the wafer and bifaciality. Also low-cost screen printed cells can yield over 20% efficiency. When combined with MWT technology, high-power back-contact modules result, which can employ very thin cells.

We report a cell conversion efficiency of 20.5% (in-house measurement, certification pending), a significant gain compared to our earlier work. We will discuss performance of thin cells relative to thicker cells, comparing experimental results to modeling.

Recently, two aspects of (mainly p-type) MWT technology have received increased attention: paste consumption and performance under reverse bias. We will discuss MWT paste consumption, showing how MWT technology, like multi-busbar technology, can support very low paste consumption. We also report on behavior of cells and modules under reverse bias. We also discuss the robustness of MWT technology to dissipation in hot spots under reverse bias.

Finally, full-size modules have been made and cell-to-module ratios of the different I-V parameters were analysed. Modules from cells with average efficiency over 20% are pending.

This work shows that low-cost n-type bifacial cells are suitable for industrial high efficiency back-contact technology.

Key words: metal wrap through; MWT; n-type silicon; back-contact

1. INTRODUCTION

High efficiency, ease of industrialization and reliability are the main drivers towards low-cost (€/Wp) Silicon PV. The International Technology Roadmap for PV expects the share of rear contact technology to take off rapidly in 2013-2014, and reach 40% in 2020. In accordance with this expected trend, the ECN's n-type Metal-Wrap-Through (n-MWT) technology is a relatively small step from the n-type front-and-rear contact and bifacial Pasha technology (developed by ECN and produced by Yingli under the brand name Panda cells [1]) to a high-efficiency rear-contact cell and module technology which offers significant cell and module performance gain in a cost-effective way [2]. With only modest changes to the n-Pasha production process, the n-MWT technology reproducibly increases the performance with up to 3% power gain at module level demonstrated [2] and up to 5% module power gain anticipated. A full size module made using n-MWT cells of 19.6% average efficiency resulted in a power output close to 280W (despite some Isc-mismatch). To place in perspective, with cell efficiency over 20%, a full area n-MWT module efficiency above 18.5% is expected.

Apart from being a cost-effective high-efficiency PV technology, n-MWT technology is also a bridge or step in the roadmap from n-Pasha to n-type IBC (interdigitated back contact) technology. Recently ECN has presented n-type IBC mercury cells [17], that employ a relatively conductive Front Floating Emitter to avoid electrical shading issues present in conventional FSF IBC cells, resulting in relaxed demands on the geometrical resolution in the processing. This allows processing of efficient solar cells (no metal at the front side) with n-Pasha type technology and a process complexity similar to n-pasha and n-MWT cells. The IBC Mercury design can be combined with ECN's back-contact module technology (see below) similar to the n-MWT cells. The IBC Mercury cells are also presented in this conference [18].

ECN's MWT module technology is based on an integrated conductive interconnection back-foil and allows to reduce cell-to-module power loss compared to a conventional tabbing technology, as used to interconnect the n-Pasha cells. Also, the module manufacturing based on integrated back-foil can be done with higher yield and reduced interconnection-process-related stress, allowing use of (much) thinner cells and therefore offering additional cost reduction possibilities. Our latest results in this paper therefore include wafers of varying thickness. In addition to efficiency and cost improvements, module reliability is important. One of the technical requirements of PV modules according to the standard IEC61215 is to pass the hot spot endurance test. Higher cell efficiencies in

combination with a trend towards 72-cell modules tend to increase power dissipation in hot spots, if those occur. Consequently, thorough investigation of cell and module reverse current characteristics must be part of the industrialization process.

In this paper, the latest results of the n-MWT technology development will be discussed. In a direct comparison run between n-MWT and n-Pasha, a 0.15% abs. efficiency gain was obtained for n-MWT over n-Pasha, giving 20.04 versus 19.89% average efficiency, respectively. In a recent n-MWT run including process adjustments, a best cell efficiency of 20.5% was obtained on n-MWT (certification pending). Routes for further efficiency increase will be discussed in this paper. Since back contact module technology allows the use of very thin cells, comparison of n-MWT cells of varying thickness is relevant: processing of n-MWT cells from 140 μ m thin mono-crystalline silicon Cz wafers (before texturing process) was therefore investigated. Only a small loss (1% of I_{sc}) was found for the thin cells, in principle not even significant within the experimental scatter, but in agreement with cell modelling.

In addition to the latest cell results and effect of wafer thickness, in this paper focus will be on reverse characteristics of the n-MWT cells and module reliability aspects related to I_{rev} . Potentially adverse effects of leakage current on n-Pasha and n-NWT single-cell laminates were investigated for a range of reverse currents. Distribution of power dissipation under reverse bias voltage and effect of leakage current in n-MWT cells were investigated by thermal imaging and direct reverse current measurement. Attention was paid to possible instability of cell parameters after prolonged reverse bias in light of recent reports on this effect [3], which we found to be not severe. Interestingly, also, MWT modules were found to be more tolerant to a given level of leakage current under reverse bias than front contact tabbed modules.

2. MWT CONCEPT FOR N-TYPE MATERIAL

2.1 Benefits of combining MWT technology with n-type material

MWT technology presents several advantages over the standard H-pattern cell technology. Apart from the current gain due to reduced front-side metallization coverage, integration into a module is easier as the cell is fully back-contacted. The mechanical stress induced on the cells by conductive adhesive based interconnection (used in our MWT modules) is low, and as a result, the breakage is reduced. Consequently, thinner and larger cells can be interconnected without yield loss. In addition, the packing density can be significantly increased. The front side metal grid benefits from a small unit cell pattern allowing large cells (cf. fig. 1). The cell interconnection based on an interconnection foil with integrated Copper or Aluminium conductor layer can be optimized for low series resistance losses and significantly reduced efficiency loss from cell to module, since the constraints related to normal front-to-back tabbed interconnection (i.e., shading loss and series resistance from the tab, and stress on the cell) are absent [4].

In addition to the efficiency enhancement due to MWT layout, performance can be increased using silicon base material with improved electrical properties. In that respect, n-type wafers generally allow (much) higher lifetimes than p-type wafers [5,6]. In contrast to boron-doped p-type material, boron-oxygen complexes are absent in n-type material. Therefore it will not suffer from lifetime degradation due to formation of a boron-oxygen related metastable defect upon illumination [7,8]. Also, n-type silicon has been proven to have a higher tolerance to common transition metal impurities [9,10]. In practice, lifetimes of several milliseconds are readily obtained in n-type Cz. The n-Pasha cells developed by ECN, Yingli Solar and Amtech (and daughter company Tempres) and brought into production by Yingli Solar, use a bifacial design with passivated front and rear side and H-pattern contact grids [1]. In addition to benefiting from high base diffusion length, this cell design has other advantages, in particular, significantly improved rear side optical and electrical properties, compared to standard p-type cells. So far, a best cell efficiency of 19.49% (independently confirmed by Fraunhofer ISE) in trial production [11,12] and 20.1% in production have been reached. Recently, efficiencies of 20.5% were obtained at ECN's pilot line [1].

MWT cell process technology in general remains close to conventional front contact cell processing, and the simplicity of the rear-side contact pattern of the MWT cells allows large tolerance regarding print alignment. The cell structure comprises a front side emitter and therefore will be less sensitive to material quality variations than back-contact back-junction cell designs. Also, integrated MWT cell and module technology has already proven itself for p-type technology.

2.2 Approach to cell process development

The n-type MWT process is very similar to the industrial process used for n-Pasha cells. Laser processing is used to form via-holes by which the front side metal grid is wrapped through the wafer. Like the n-Pasha cells, the cell structure comprises a front-side boron emitter, a phosphorous Back Surface Field (BSF) and an open rear side metallization suitable for thin wafers. Metal contacts are deposited by industrial screen-printing process with no further requirements regarding alignment compared to the screen-printing process used in the industrial n-Pasha process. The front and rear side metal grid patterns are based on a H-pattern lookalike grid design, combined with the unit cell concept [13]. We have chosen a H-pattern lookalike grid because it is well suited for a comparison of losses between n-MWT and n-Pasha cells. As module interconnection of n-MWT cells does not require tabs on the front of the cells, the front side busbars can be significantly slimmed down compared to conventional n-Pasha cells. As a result, total shading losses are reduced. Correspondingly, however, resistance in the busbars affects the total series resistance of the cell. Shading and resistance losses are balanced to increase power output of the n-MWT cells compared to the n-Pasha cells. The front and rear sides of the cells made according to this process sequence can be seen in Fig. 1.

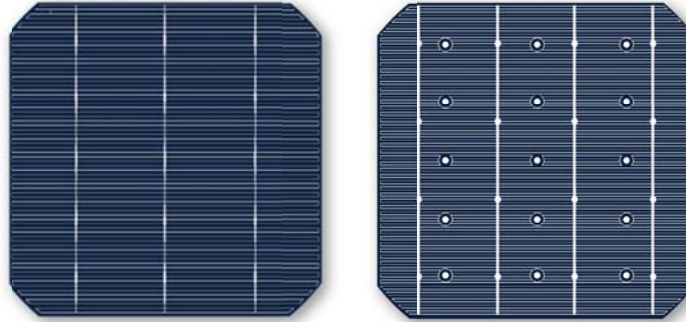


Fig. 1. Example of n-type MWT silicon solar cells (239cm^2) with a H-pattern based unit cell design with 3×5 via's and 31 contact points for module interconnection: left picture front side and right picture rear side.

3. N-MWT CELL EFFICIENCY

3.1 Efficiency gain of MWT over front-and-rear-contact cells

n-type MWT and n-type Pasha solar cells were prepared from adjacent n-type Cz wafers (239cm^2 , $200\ \mu\text{m}$ thickness, around $1.7\ \Omega\text{cm}$ resistivity). Both groups were processed in parallel and received identical texture (random pyramids formed by alkaline etching), emitter and BSF profiles, passivation, SiNx anti-reflective coating (ARC), metal pastes for emitter and BSF contacts, and firing. I/V data are presented in Table 1.

Table 1. I/V characteristics of n-type Pasha cells and n-type MWT cells with comparable J_0 and metallization parameters, to illustrate the relative changes associated with MWT design. R_{se} obtained from fit to two-diode model. J_{sc} corrected for spectral mismatch. N-type Pasha and n-type MWT measurement chucks have a reflective surface to simulate the operation in a module with white back sheet. (* indicates slight FF overestimation due to shorting of the n-Pasha rear grid on the electrically conductive measurement chuck.)

	J_{sc} (mA/cm^2)	V_{oc} (mV)	FF (%)	η (%)	R_{se} ($\text{m}\Omega$)
Av. on 12 cells					
n-Pasha	38.90	652	78.4*	19.89	4.9
n-MWT	39.95	652	76.8	20.04	5.7
Best efficiencies					
n-Pasha	38.97	653	78.5*	19.98	4.8
n-MWT	40.01	653	77.0	20.10	5.6

The J_{sc} gain of 2.6% for the n-MWT cells is related to the reduced front metal shading losses thanks to the narrower front busbars. Because the n-Pasha process used non-contacting front busbar paste [1], there results no V_{oc} gain of the n-MWT cells from the reduction of busbar area (reduced metal recombination). In this experiment the cell efficiency benefit of the MWT structure is therefore about $0.15\%_{\text{abs}}$, compared to about $0.25\%_{\text{abs}}$ previously reported. The major contributions to series resistance and FF losses are summarized in Table 2.

Table 2. Calculated contributions to series resistance and FF losses of the n-MWT cells compared to the n-Pasha cells.

Source of R_{series} in MWT cell	R_{series}	FF loss
Metal via resistance	0.2 m Ω	0.3% abs.
Front side busbars	0.7 m Ω	1.1% abs.
Increase of I_{sc}		0.1% abs.
Total	0.9 m Ω	1.5% abs.

3.2 Improved cell process

The MWT process was recently adjusted to obtain a higher FF. One aspect of this improvement was an improvement of design and conductivity of the front and rear side grid metallisation, resulting in about 1%abs FF-improvement. From other improvements another 1%abs FF-gain was obtained. As a result, the efficiency increased to 20.5% (in-house measurement, J_{sc} corrected for spectral mismatch, certification pending) as shown in Table 3.

Table 3. I/V characteristics of n-type MWT cells with improved processing. Other details as in Table 1.

	J_{sc} (mA/cm ²)	V_{oc} (mV)	FF (%)	η (%)	R_{se} (m Ω)
Average of 60 n-MWT cells	39.8	649	78.5	20.3	2.3
Best efficiency n-MWT	39.8	650	79.2	20.5	2.3

4. IMPROVING MWT EFFICIENCY THROUGH THE NUMBER OF CONTACT POINTS AND COMPARISON WITH MULTI-BUSBAR CELLS

Several options exist to reduce the FF loss of n-MWT cells relative to n-Pasha cells. A straightforward option is increasing the number of vias. However, this may also increase recombination, and therefore, cause V_{oc} loss as illustrated in Fig. 2. Therefore, for typical device parameters we expect a maximum efficiency increase of around 0.2% absolute when using an optimum of about 55 via-holes, compared to the present number of 16 via-holes.

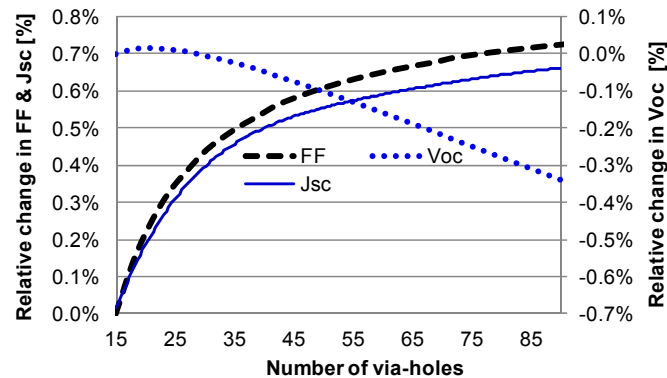


Fig. 2: Calculated relative FF, shading and V_{oc} changes as a function of the number of via-holes for n-MWT cells

More importantly, increasing the number of vias allows to reach similar or better benefits of paste reduction as in multi-busbar cells. For example, 5 rows of vias provide the same opportunity for paste reduction as a solar cell with 5 busbars. In fact, the relative efficiency gain of MWT over Pasha cell designs increases slightly with the number of via-rows / busbars. Further gain is possible by using other metallisation grid patterns than the rectangular H-pattern grid. For the rear, contact pads can be added without increasing the number of vias, almost without effect on recombination, again resulting in reduction of metallisation paste and resistive losses. We estimate that increasing the number of vias and contact points by approx. a factor of 2 should enable reductions of paste consumption also by approx. a factor 2, even in combination with an increase of cell efficiency.

We have analysed the efficiency change of an n-MWT cell as a function of the type of front-side pattern (H-pattern as shown in Fig.1 or ECN's "Star"-pattern from which a unit cell is shown in Fig. 3), the number of holes and the front metallisation properties. The results are presented in table 4. The absolute efficiency change includes the effect of the number of contact points and metallisation coverage on the Voc, Isc and pseudo-FF.

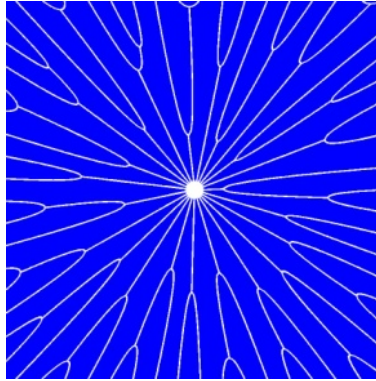


Fig. 3. Schematic of a star-pattern unit cell

Table 4. Absolute efficiency change of an n-MWT cell calculated for different front side pattern (H-pattern or Star-pattern), different number of via-holes (up-to 25) and different front metallisation properties. (W_{line} is finger width, R_{line} is finger line resistance)

Front pattern type	Number of holes	Metallisation area (%)	Assumed front metallisation properties	Calculated absolute efficiency change
5x5 Star-pattern (reference)	25	3.6	$W_{line} = 56\mu\text{m}$ $R_{line} = 0.23 \Omega/\text{cm}$	0.00%
5x5 Star-pattern	25	4.2	$W_{line} = 70\mu\text{m}$ $R_{line} = 0.5 \Omega/\text{cm}$	-0.30%
4x4 Star-pattern	16	3.6	$W_{line} = 56\mu\text{m}$ $R_{line} = 0.23 \Omega/\text{cm}$	-0.03%
4x4 star pattern	16	4.5	$W_{line} = 70\mu\text{m}$ $R_{line} = 0.5 \Omega/\text{cm}$	-0.40%
5x5 H-pattern	25	4.3	$W_{line} = 56\mu\text{m}$ $R_{line} = 0.23 \Omega/\text{cm}$	-0.30%
5x5 H-pattern	25	4.9	$W_{line} = 70\mu\text{m}$ $R_{line} = 0.5 \Omega/\text{cm}$	-0.50%
4x4 H-pattern (currently used)	16	4.6	$W_{line} = 56\mu\text{m}$ $R_{line} = 0.23 \Omega/\text{cm}$	-0.40%
4x4 H-pattern (currently used)	16	5.1	$W_{line} = 70\mu\text{m}$ $R_{line} = 0.5 \Omega/\text{cm}$	-0.60%

From this study, the best efficiencies will be reached using the Star-pattern. Compared to the H-pattern currently used (H-pattern, 16 holes) the Star-pattern with 25 holes, in case of similar line properties, will allow to improve the efficiency by around 0.3-0.4% absolute while reducing paste consumption (metallisation area) by about 20%. The H-pattern design involves a busbar to connect the fingers to the via-holes. Increasing the number of holes will therefore reduce the busbar length and the distance to the via-holes for the charge collected in this busbar, as well as the current collected per unit cell. Consequently, an efficiency gain of around 0.1% will be obtained by increasing the number of holes from 16 to 25, again in combination with a reduction of paste consumption (however, more modest than in the case of the Star pattern). The efficiency gain calculated for the Star-pattern grid is negligible when going from 16 to 25 holes.

Similar efficiency benefits and larger paste reductions can be obtained by using more contact points on the rear of the cell, giving rise to the estimated feasibility of a factor 2 reduction of paste consumption mentioned above.

5. N-MWT MODULE POWER

We have previously extensively reported on n-MWT module performance compared to n-Pasha module performance, and in particular comparative cell-to-module losses [2]. Compared to the front to rear side tabbed interconnection used for the n-Pasha cells, the rear-side foil interconnection of the MWT module allows to reduce the module series resistance by using more interconnect metal (more cross-sectional area) and thereby reduce the cell to module FF loss. An n-MWT module outperforms the corresponding n-Pasha tabbed module with a CTM FF loss which can be below 0.8% absolute, more than 3 times lower than the FF loss for n-Pasha as shown in table 5.

Table 5: n-type MWT and n-type Pasha average cell efficiency, corresponding module power and FF loss from cell to module (multi-flash class A, IEC60904-9 measurement, ESTI reference module)

	Average cell η	P_{max} (W)	cell-to-module FF loss
n-MWT module	18.9%	273	0.8%
n-Pasha module	18.6%	265	3%

In the period between the fabrication of first n-MWT module and the latest results discussed in section 3, a batch of 60 n-MWT cells were fabricated according to a process at an intermediate phase of improvements [1]. This process being less optimal than it is today, the average cell efficiency presented in Table 3 is somewhat lower than the one presented in section 3. For this n-MWT module, back sheet with improved reflectivity was used. The n-MWT module I-V parameters were measured at ECN using a class A multiflash tester (16-flash measurement). Maximum power and absolute FF loss from cell to module are also presented in Table 6.

Table 6: n-type MWT average cell efficiency, corresponding module power and FF loss from cell to module (multi-flash class A, IEC60904-9 measurement, ESTI reference module)

	Average cell η	P_{max} (W)	cell-to-module FF loss
n-MWT module	19.6%	279	1.3%

Despite an improved maximum power, this n-MWT module shows a slightly higher CTM FF loss compared to the n-MWT module presented in section 4a which is possibly due to the use of a different conductive adhesive. Also, the module I_{sc} turned out to be lower than expected from results on earlier modules, because of I_{mpp} mismatch of a few n-MWT cells. This will also have contributed to a reduced module FF. With better I_{mpp} matching, the CTM FF-loss of Table 5 and cell efficiency above 20% as demonstrated in section 3, module power above 290Wp is within reach. N-MWT modules with such specifications are currently in preparation.

6. PROCESSING OF 120 μ M THIN N-MWT CELLS

In addition to the reduced cell-to-module power loss, the ECN's MWT module technology exerts less stress during interconnection allowing use of thinner cells and therefore offering a significant cost reduction opportunity. Therefore we compared cells from 140 μ m and 200 μ m n-type Cz wafers thickness with similar electrical properties (bulk lifetime and diffusion length) and processed in parallel. Average I/V data are presented in Table 7.

Table 7. I/V characteristics of n-type MWT cells processed from 200 μ m and 140 μ m thin wafer. Details as in Table 1.

	J_{sc} (mA/cm ²)	V_{oc} (mV)	FF (%)	η (%)	I_{rev} (A @ -12V)	R_{se} (m Ω)
Av. on 12 cells						
n-MWT-200 μ m	39.95	652	76.8	20.04	<0.3	5.7
n-MWT-140 μ m	39.63	651	76.5	19.74	<0.3	5.8

No increase in breakage rate was observed during the processing of these thin MWT cells at ECN. Comparable V_{oc} and FF show that there is no significant shift between bulk and surface recombination. A \approx 1% relative lower J_{sc} for the thin n-MWT cells is probably due to reduced light trapping. This effect is illustrated by the higher reflectance at the long wavelengths as shown in Fig. 4. This also correlates with the lower IQE of the thin n-MWT cell for wavelengths of 1000nm and longer (due to the rear internal reflection being less than 100%). These results are consistent with PC1D modelling of our cells. However, we note that fluctuations of 1% in J_{sc} between cells from nominally good material quality can occur anyway, even for standard thickness wafers. Therefore it is difficult to draw firm conclusions on the effect of wafer thickness on J_{sc} at this moment.

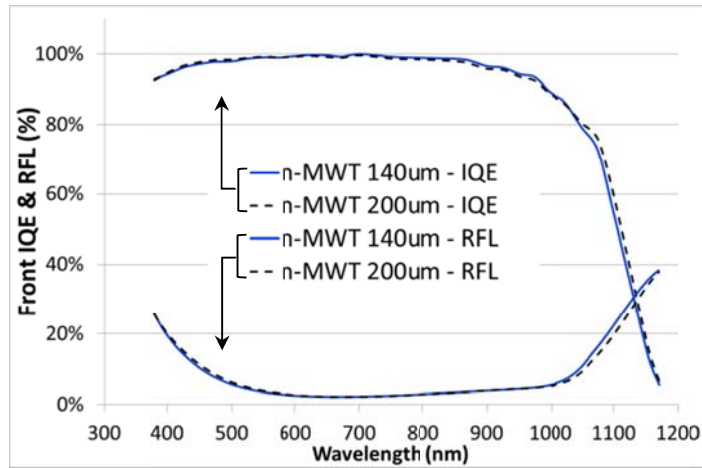


Fig. 4. Internal quantum efficiency and Reflectance measured from the front side of n-MWT cells processed from 200 μ m and 140 μ m wafer thickness.

7. REVERSE BIAS BEHAVIOUR OF CELLS

The reverse characteristics in the dark of our n-MWT cells are normally very satisfactory (well below 0.5A). Table 7, for example, shows the average I_{rev} (at 12V reverse bias) obtained in a recent experiment. Since there have been reports about instability of cell parameters after reverse biasing [3] in this section we present results on the stability of cell characteristics in some detail.

Four n-MWT cells with different initial values of reverse current (I_{rev}) were selected (0.1A, 0.5A, 1A and 9A at -12V) to study stability of the reverse characteristics in dark. Each cell was exposed to a reverse voltage of 12V in the dark for up to one hour. Electro-luminescence images as well as dark I/V characteristics, both under reverse voltage bias, were acquired at regular time lapses. In this initial study, the cells were placed in the dark on a metal chuck (without active cooling system but with large thermal mass). This is not fully representative for the conditions in the field regarding temperature fluctuations as the metal chuck by itself is most likely a better heat dissipater than the conductive back sheet foil used in an MWT module. However, results of a similar study performed on single-cell laminates are described in the next section.

Fig. 5 shows an example of an electro-luminescence measurement under reverse bias performed on an n-MWT cell with high I_{rev} characteristics (9A at -12V). When exposed to a reverse bias voltage of 12V, the current flows through a (non-linear) shunt or junction breakdown resulting in light emission in the visible wavelength range [15]. The light intensity is proportional to the level of reverse current. As visible in Fig. 5, particularly on the zoom-in, intense light escapes from the rear-side metal pad edges. This indicates that the high reverse current for this MWT cell originates from a shunt or junction breakdown located at the interface between the metal pad, connected to the front side grid, and the n-type base silicon area around the via-hole which is un-diffused. The type of shunt or junction breakdown has not been identified yet. In the case of low reverse current n-MWT cells (<0.5A at -12V), no emitted light is visible when exposed to a reverse voltage of 12V.

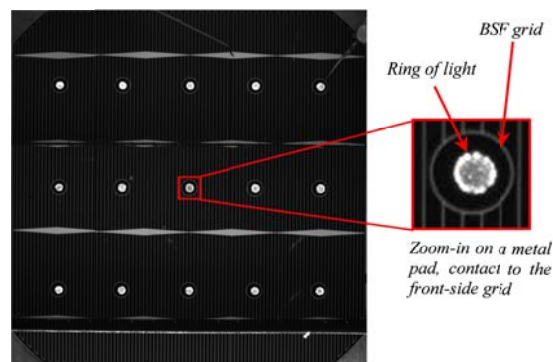


Fig. 5: Grey scale electro-luminescence image of the rear-side of a high I_{rev} n-MWT cell (9A at -12V) under 12V reverse voltage bias. The rear side includes 15 metal pad-contacts to the front side grid (through the via-holes) and 16 diamond-shaped contacts to the base. A zoom-in centered on a metal pad is presented at the right side of the main picture where a ring of light around the metal pad is clearly visible

Relative changes of I_{rev} level measured at -12V for one hour of exposure at a voltage load of -12V are shown in Fig. 6. Relative changes of I_{rev} are plotted for the four selected n-MWT cells.

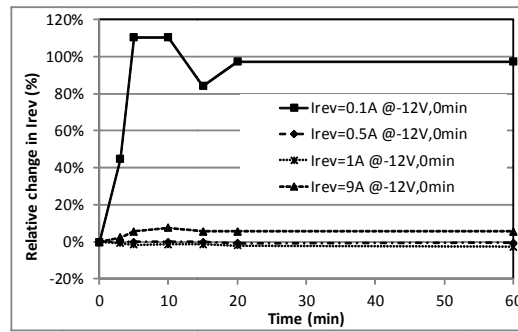


Fig. 6. Relative changes of dark reverse current measured at -12V as a function of exposure time under a reverse voltage of 12V for four n-MWT cells having different initial reverse current values (0.1A, 0.5A, 1A and 9A at -12V).

From these measurements, two different behaviours independent from the initial I_{rev} values of the cell can be distinguished. For some cells, the reverse current level remains stable over time and can even slightly decrease (case of the cells with initial reverse current of 1A and 0.5A at -12V). For other cells, the reverse current increases within the first 10 minutes to subsequently slightly decrease and stabilize (case of the cells with initial I_{rev} of 9A and 0.1A at -12V). Despite the large relative reverse current increase of 110% measured for the cell with 0.1A initial I_{rev} , its I_{rev} level remains below 0.2A after stabilization. Because absolute reverse current fluctuations under reverse bias remain small, no changes in the electro-luminescence images were detected. Within the noise we found no noticeable change of slope at zero voltage, i.e., no change of forward shunt of the cells. Many more tests like these have been performed and are still going on, and so far these results of stable I_{rev} (after perhaps an initial limited increase) are typical.

8. REVERSE BIAS BEHAVIOUR OF MODULES

Effect of leakage current in n-MWT and n-Pasha laminates was investigated by thermal imaging as described in [16]. Degradation of the laminates was assessed by visual appearance and by the I/V power output. The laminates were exposed to a reverse voltage of 10V for up to one hour in the dark at a base temperature of 50°C.

N-MWT and n-Pasha cells with I_{rev} ranging from 0.5A to 8A were selected. Example of IR images of the corresponding n-MWT and n-Pasha laminates with I_{rev} of 2.5A are shown in Fig. 7. Typically in n-Pasha cells one or two single hot spots are visible. In contrast, in n-MWT cells, the current may flow mainly through the via-holes as also shown in Fig. 7 (although of course also patterns as for the n-Pasha cell may be present).

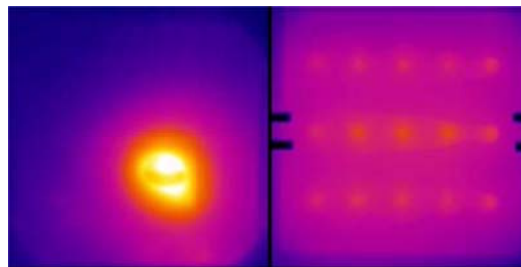


Fig. 7. IR images of laminates with I_{rev} of $\approx 2.5A$ at -10V, showing n-Pasha(left) and n-MWT (right). The IR scale ranges from 40°C (black) to 160°C (white)

The MWT laminate exhibits a lower maximum temperature. A reverse current of 2.6A can be sufficient to cause visual damage and efficiency loss for an n-Pasha laminate while the n-MWT laminate remains undamaged. We believe this is because the reverse power dissipation in the n-Pasha laminates is concentrated, while it is distributed in the n-MWT laminates. The full copper back foil used to interconnect the n-MWT cells is likely to help the heat dissipation. In this respect we are

now further studying the effect of a copper back-foil on the heat dissipation by hot spot patterns typical for n-Pasha cells (which may also occur in n-MWT cells).

9. CONCLUSION

We have developed a manufacturing process for metal-wrap-through silicon solar cells and module on n-type mono-crystalline Czochralski (Cz) silicon wafers, leading to a module power, so far, of 279Wp from cells of 19.6% average efficiency. With current density (J_{sc}) of about 40 mA/cm² and open circuit voltages above 650 mV, the large area (239 cm²) n-MWT solar cells outperform n-Pasha solar cells (bifacial n-type H-pattern cells with contact grids on front and rear) manufactured with a comparable process. In a recent direct comparison experiment, an efficiency gain of 0.15% absolute for MWT was achieved with a best MWT cell efficiency of 20.5%. Even higher cell efficiency is expected by improving the cell contacting layout (e.g grid pattern, number of via holes, busbars and contact pads) which will also provide opportunity for paste reduction.

Performance enhancement at module level is obtained thanks to the ECN MWT module manufacturing technology based on integrated back-foil (conductive interconnect patterns integrated on the backfoil). In a full size module (60 cells) comparison experiment between MWT and equivalent n-Pasha tabbed modules, a power increase of approximately 3% for the n-MWT module was obtained. Interconnection of a batch of cells with average efficiency of 19.6% resulted in a module power close to 280Wp. Module power gain above 290Wp is expected to be reached by better I_{mpp} matching, further optimization of the back-sheet reflectivity, and use of cells with efficiency above 20%. This work is currently being conducted.

Successful processing of 140 μ m thin (initial thickness) n-MWT cells was demonstrated: low breakage rate (similar to standard thickness cell processing), and a small J_{sc} loss of 1% compared to standard thickness n-MWT cells. This small J_{sc} loss, as well as IQE and reflection measurements, match PC1D modeling of lower light coupling inherent to the wafer thickness. These results together with the low interconnection stress of the ECN's MWT technology add another possibility to reduce cost of the technology.

Stability of the dark reverse as well as illuminated I/V characteristics of n-MWT cells after prolonged reverse bias voltage was found to be satisfactory, independently from the level of initial reverse current. Despite a brief rise of the reverse current in the first minutes of reverse bias in some cases, stability is rapidly reached. Reverse voltage in MWT-back contact modules typically causes less thermally-induced damage than in n-Pasha modules with similar I_{rev} , thanks to more optimum distribution of the power dissipation over the via-holes (if those are the main leakage locations) and dissipation by the metal back-foil. This latter benefit needs to be investigated further.

7 ACKNOWLEDGMENTS

This work has been partially funded by RVO (former AgentschapNL) within the International Innovation program under the grant agreement no. OM092001 (Project FANCY). Also part of the research leading to these results has received funding from the European Union's Seventh Programme for research, technological development and demonstration under grant agreement No 308350. This paper reflects only the authors' views and the European Union is not liable for any use that may be made of the information contained herein. We also gratefully acknowledge collaboration with Tempres Systems.

8 REFERENCES

- [1] I.G. Romijn, Front side improvements for n-Pasha solar cells, SNEC conference, 2014.
- [2] N. Guillevin et al., 27th EU-PVSEC, 2012.
- [3] E. Lohmüller et al, 27th EU-PVSEC, 2012.
- [4] several contributions at the MWT workshop 2013, Freiburg, Germany, Nov 20-21, 2013, unpublished
- [5] S. Martinuzzi et al., Pogr. Photovolt.: Res. Appl., 2009. 17: p. 297.
- [6] A. Cuevas et al., Appl. Phys. Lett. 2002, 81: p. 4952.
- [7] J. Schmidt et al., Proc. 26th IEEE PVSC, 1997, p. 13.
- [8] S. Glunz et al., 2nd WCPEC, 1998, p. 1343.
- [9] D. Macdonald and L.J. Geerligs, Appl. Phys. Lett., 2008, 92: p. 4061.
- [10] J.E. Cotter et al., 15th Workshop on Crystalline Silicon Solar Cells & Modules, 2005, p. 3.
- [11] Yingli press release Oct 20, 2010, obtained in trial production lines. Independently verified at ISE.

- [12] Yingli press release Feb 18, 2011. Best efficiency in production lines.
- [13] A.R. Burgers et al., *Solar Energy Materials & Solar Cells*, 2001, 65: p. 347.
- [14] N. Guillemin et al, CPTIC SolarCON Shanghai, 2012.
- [15] Obeidat et al., *Appl. Phys. Lett.*, Vol. 70, No. 4, 27 January 1997.
- [16] M.J. Jansen, PVSEC-22 Photovoltaic Science and Engineering Conference, Hangzhou, China, 5-9 November 2012.
- [17] I. Cesar et al. "Mercury: A Back Junction Back Contact Cell With Novel Design For High Efficiency And Simplified Processing", *Energy Procedia*, 4th Int. Conf. on Silicon Photovoltaics, Silicon PV 2014.
- [18] I. Cesar et al. "Mercury: A Back Junction Back Contact Cell With Novel Design For High Efficiency And Simplified Processing", SNEC conference, Shanghai, May 2014